HHS Public Access

Author manuscript

Pain. Author manuscript; available in PMC 2021 May 01.

Published in final edited form as:

Pain. 2020 May ; 161(5): 949–959. doi:10.1097/j.pain.0000000000001781.

Recovery from nerve injury induced behavioral hypersensitivity in rats parallels resolution of abnormal primary sensory afferent signaling

M. Danilo Boada, MSc, PhD[a], **Thomas J. Martin, PhD**[a], **Renee Parker, BA**[a], **Timothy T. Houle, PhD**[b], **James C. Eisenach, MD**[a], **Douglas G. Ririe, MD, PhD**[a]

[a]Pain Mechanisms Lab, Department of Anesthesiology, Wake Forest School of Medicine, Winston-Salem, North Carolina, USA

[b]Department of Anesthesiology and Perioperative Medicine, Harvard Medical School, Massachusetts General Hospital, Boston, MA, United States.

Abstract

Pain and hypersensitivity months after peripheral injury reflect abnormal input from peripheral afferents likely in conjunction with central sensitization. We hypothesize that peripheral changes occur in defined sensory afferents and resolve as behavioral response to injury resolves. Male Sprague Dawley rats underwent sham or partial L5 spinal nerve ligation and paw withdrawal threshold was sequentially measured during recovery. At 2, 4, 8, and 12 weeks after injury randomized animals underwent electrophysiologic assessment of L4 fast conducting high and low threshold mechanoreceptors and individual neuronal mechanical thresholds were contrasted with paw withdrawal thresholds in the same animals. Paw withdrawal thresholds decreased after injury and resolved over time ($p<0.001$). Similarly, mechanical thresholds of fast conducting high threshold mechanoreceptors decreased after injury and resolved over time ($p<0.001$). In contrast, mechanical thresholds of low threshold mechanoreceptors increased after injury and resolved over time ($p<0.001$). Distributions of recordings from each afferent subtype were perturbed after injury and this too resolved over time. After resolution of behavioral changes, several electrical abnormalities persisted in both neuronal subtypes. These data extend previous findings that mechanically sensitive nociceptors are sensitized whereas tactile, largely Aβ afferents, are desensitized after nerve injury by showing that the time course of resolution of these changes mirrors that of behavioral hypersensitivity in a surgical injury including neural damage. These data support a role of abnormal peripheral input, from both nociceptor and tactile afferents, during recovery from peripheral injury and underscore the potential importance of both classes of afferents as potential targets for pain treatment.

Corresponding Author: Douglas Ririe, MD, PhD, Department of Anesthesiology, Wake Forest School of Medicine, Medical Center Boulevard, Winston-Salem, NC 27157-1009, Ph: 336-716-4498 Fax: 336-716-8190 dririe@wakehealth.edu.

Competing Interests

JCE has consulted in the past 3 years to Adynxx in the development of treatments to speed recovery from pain after surgery.

The other have no conflicts of interest to report.

Institutional Address: https://school.wakehealth.edu/

1. Introduction

Pain from surgery is initially dominated by peripheral nociceptive afferent input [10]. This nociceptive afferent activity reflects both direct afferent axonal injury and locally released substances, in part inflammatory in nature, which modulate neuronal activity impacting neuronal sensibility and tissue integrity [18; 27; 37]. Recovery from postoperative pain reflects in part the degree and location of nerve injury with pain from superficial surgery resolving along with local tissue healing. In contrast, more extensive nerve injury results in ongoing activity of neurons that carry nociceptive information or modulation of input of nociceptive information that is arriving and being integrated at the level of the spinal cord independent of tissue integrity [39]. Central sensitization can also participate in pain after injury and has been postulated to be a determinant of slowly recovering or persistent pain after surgery [42]. At the extreme, this view posits that in chronic postsurgical pain the peripheral input returns to normal or near normal, but this input is interpreted as nociceptive because of persistent central sensitization. Clinical studies showing pain relief in patients with chronic pain by peripheral local infiltration of lidocaine indicate that peripheral input is critical, but do not distinguish whether this input is normal or abnormal [20].

Classically, acute post-surgical pain is thought to result from physical mechano-activation of nociceptors (high threshold peripheral sensory neurons) and hypersensitivity is thought to reflect increased sensibility of nociceptors that innervate the damaged area [11]. We previously reported that nerve injury and incision both result in sensitization of the fast conducting high threshold nociceptors (AHTMR) and desensitization of fast conducting low threshold mechanoreceptors (LTMR) [4; 5]. The time course of resolution of nociceptor sensitization and the changes in non-nociceptive afferent neurons over time are not well elucidated. There is increased sensitivity of the AHTMR that correlates with the degree of reflexive behavioral hypersensitivity and non-reflexive pain behavior after injury [8; 9]. The increased sensitivity of AHTMRs is consistent with the literature while the desensitization of LTMRs has been largely unappreciated. While this may seem to be of secondary importance with respect to the perception of pain, the desensitization of the LTMR may be a valuable component for understanding and treating persistent pain and improving or accelerating resolution of pain and return to full function.

In this study we hypothesize that both AHTMR and LTMR sensibilities are changed acutely after surgery and resolve towards normal during resolution of behavioral hypersensitivity in rats. Single cell receptive field responses in phenotypically characterized neurons over time after partial nerve injury of the L5 spinal nerve (pSNL) are used to evaluate this time dependent relationship during the resolution of the behavioral withdrawal response to injury and to determine the relationship of resolution of the withdrawal behavior with the resolution of the changes in LTMRs and AHTMRs. This should serve to better understand peripheral afferent activity and its relationship with behavior as a result of nerve injury and during resolution.

2. Methods

2.1. Animals

Seventy-four juvenile male Sprague-Dawley rats (6 weeks at the time of surgery) were used (Envigo, St. Louis, MO). Animals were housed together in pairs, in a climate-controlled room under a 12-h light/dark cycle in AAALAC approved facilities. The use and handling of animals were in accordance with guidelines provided by the National Institutes of Health and the International Association for the Study of Pain and received approval from the Institutional Animal Care and Use Committee of the Wake Forest University Health Sciences and all experiments performed during the dark phase of the light:dark cycle.

2.2. L5 partial spinal nerve ligation (pSNL)

The pSNL was performed in 43 animals. Animals were deeply anesthetized with isoflurane and, under aseptic conditions, the skin was incised at the midline over the lumbar spine. The right L5 spinal nerve was identified and approximately 1/3–1/2 thickness of the L5 spinal nerve was ligated with a 9–0 nylon suture under a dissecting microscope as previously described [22]. Care was taken not to pull the nerve or contact the intact L4 spinal nerve. After hemostasis was achieved, the muscle layer was approximated with 4–0 synthetic absorbable suture (Look, Reading, PA) and the skin closed with absorbable sutures. A sham procedure was performed in 31 animals. The surgical procedure was identical to that described above, except that the left L5 spinal nerve was not injured. After the surgery, the rats were returned to their cages, kept warm under a heat lamp, and monitored during recovery.

2.3. Experimental groups

The animals were clustered into five experimental groups with respect to completion (in weeks) after surgery at the following times: Week 2 (10 L5 pSNL and all 31 Sham), Week 4 (10 L5 pSNL), Week 8 (9 L5 pSNL), Week 12 (14 L5 pSNL). Behavioral and electrophysiological testing were performed in a consecutive manner for every animal per experimental group.

2.4. Behavioral testing

Animals were placed on a mesh surface in a plastic cage and were acclimated for 20 min before testing. Withdrawal threshold in awake rats was assessed on the hind paws resting on the mesh surface using calibrated von Frey filaments application to the footpad until the filaments bent. This was done by a person blinded to the surgical treatment. The von Frey filaments used were 3.84, 4.08, 4.31, 4.56, 4.74, 4.93, 5.18, 5.46, and 5.88 corresponding to 0.5, 0.9, 1.7, 3.7, 5.5, 8.0, 12.4, 21.5, and 53.0 grams, respectively. This was done 3 times with a positive response determined by brisk withdrawal of the paw from the filament. The force resulting in 50% probability of withdrawal (paw withdrawal threshold) was determined using the up-down method as previously described [14]. Withdrawal thresholds were determined before pSNL and weekly after pSNL until electrophysiology experiments. All animals were included in the data analysis, and no animal in the study had a wound dehiscence or infection during the study.

2.5. Electrophysiological testing

After behavioral assessment at the specified timepoint pSNL animals were randomly assigned to electrophysiology, and rats were deeply anesthetized with isoflurane 3%, tracheotomized and pressure-controlled ventilated with humidified oxygen. Heart rate was monitored throughout as a guide to depth of anesthesia, immobilized with rocuronium (1 mg/kg, s.c.) and inspired isoflurane maintained at 2% throughout the study. As illustrated in Figure 1, a dorsal midline incision was made in trunk skin and the L4 dorsal root ganglion (DRG) and adjacent spinal cord were exposed by laminectomy as previously described [7]. The tissue was continuously superfused with oxygenated artificial cerebrospinal fluid [aCSF (in mM): 127.0 NaCl, 1.9 KCl, 1.2 KH2PO4, 1.3 MgSO4, 2.4 CaCl2, 26.0 NaHCO3, and 10.0 D-glucose]. The spinal column was secured using custom clamps and the preparation was transferred to a preheated (32–34°C) recording chamber where the superfusate was slowly raised to 37°C (MPRE8, Cell MicroControls, Norfolk, VA). Pool temperature adjacent to the DRG was monitored with a thermocouple (IT-23, Physitemp, Clifton, NJ). Rectal temperature (RET-3, Physitemp) was maintained at 34 ±1°C with radiant heat.

The electrophysiological recordings from L4 DRG neurons were limited to a maximum duration of 4250 sec (70.8 min) to diminish sensitization and to allow equal time of searching for afferents in Sham and pSNL animals. DRG soma were impaled with borosilicate microelectrodes (80–250 MΩ) containing 1 M potassium acetate. Intracellular penetrations with a resting membrane potential of ≤ −40 mV were characterized further. DC output from an Axoclamp 2B amplifier (Axon Instruments/Molecular Devices, Sunnyvale, CA) was digitized and analyzed off-line using Spike2 (CED, Cambridge, UK). Sampling rate for intracellular recordings was 21 kHz throughout (MicroPower1401, CED).

In this study, both cells with Positive mechanically sensitive Receptive Field (P-RF) (L5 pSNL and sham groups) and No mechanically sensitive Receptive Field (N-RF) (L5 pSNL group only) were included. Only cells capable of generating a somatic AP (by current somatic injection, 25 and 500 ms pulses) and with impalements stable long enough to adequately explore the full extent of the skin at the L4 dermatome (>2 min) were included. Unexcitable cells (stable impalements of more than 5 min with steady Em ≥−40 mV but unexcitable to peripheral mechanical stimuli and intrasomal injection of current) were noted for general statistical purposes only.

2.6. Cellular classification protocol

To identify the RF, the skin was searched by applying gentle pressure with a fine-tipped brush. For non-responding afferents, subsequent searches used increasingly stiffer probes and finally sharp-tipped watchmaker forceps. Afferents with cutaneous RFs were distinguished from those with deep RFs by displacing skin to ensure that RFs tracked rather than remained stationary. Mechanical thresholds were characterized with calibrated von Frey filaments (Stoelting, Wood Dale, IL) with the mechanical threshold being the minimum von Frey hair producing neuronal activity. The cellular classification process was performed in a sequential manner and results of these procedures were combined with specific cellular properties (action potential [AP] shape and somatic passive characteristics) to assign every cell into one of three simplified categories: LTMR, AHTMR, CHTMR, based on the

strongest defining characteristics [6] and in order to compare afferents between sham and pSNL groups, innervating both types of skin (glabrous and hairy) [7]. Their adaptation rate (rapidly adapting [RA] or slowly adapting [SA] units) was evaluated in all cells since "on-off" responses to steady suprathreshold mechanical stimulation are characteristic of a large percentage of tactile afferents (LTMRs) and never observed in nociceptors (AHTMRs and CHTMRs) (2 sec per trial, 3 trials per cell, 2× mechanical threshold). This procedure used a micromanipulator-based probe to stretch the skin in and around the cellular RF. In addition, the application of vibratory stimuli was used to assess cellular response characteristics within the RF (tuning fork of 256 and 512 Hz; SKLAR instruments, West Chester, PA) because tracking of vibration has been shown to be 100% predictive of the LTMR population [6; 7]. In all cases, RFs were characterized and measured with the aid of a zoom stereomicroscope (for details see RF analysis section).

2.7. P-RF and N-RF neurons: somatic electrical properties

Active membrane properties of all excitable neurons were analyzed including the amplitude and duration of the AP and afterhyperpolarization (AHP) of the AP; AP and AHP durations were measured at half-amplitude (D50 and AHP50, respectively) to minimize hyperpolarization-related artifacts. Passive properties were analyzed including membrane resting potential (Em), input resistance (Ri), time constant (τ), inward rectification, and, where possible, rheobase; all but the latter were determined by injecting incremental hyperpolarizing current pulses (≤0.1 nA, 500 ms) through balanced electrodes. The value of τ was obtained from the single exponential fit to the onset phase of a small hyperpolarizing voltage response. The membrane capacitance (Cm) was estimated using the relation: $\tau = R_i \times Cm$ [12].

The N-RF cells were separated in two different populations based on the shape of the AP [4; 12; 19; 43]: neurons with inflection in the repolarizing phase (S-type neurons) and neurons without this inflection (F-type neurons). To more clearly determine the presence of this inflection, the differentiated records of the AP were used (presence or absence of a second additional negative component in the time course of the AP derivative). Since RF properties, especially response characteristics, were used to define differences in the fast conducting afferents (those without inflected APs) the ability to accurately define and categorize these two populations further was not possible.

All included cells satisfied the following requirements: resting membrane potential more negative than −40 mV, AP amplitude ≥30 mV and the presence of AHP. Passive membrane properties indicative of poor (extremely low Ri and/or Tau) impalement were also reasons for exclusion.

2.7.1 P-RF neurons only: CV—Because intact lumbar DRGs serve multiple nerves, spike latency was obtained by stimulating the RF at the skin surface using a bipolar electrode (0.5 Hz); this was performed following all-natural stimulation to prevent potential alterations in RF properties by electrical stimulation. All measurements were obtained using the absolute minimum intensity required to excite neurons consistently without jitter; this variability (jitter) in the AP generation latency (particularly at significantly shorter

latencies), seen at traditional (i.e., two- to three-fold threshold) intensity has been presumed to reflect spread to more proximal sites along axons. Any neuron with jitter was rejected (3 cells). Stimuli ranged in duration from 50 to 100 μs; utilization time was not considered. Conduction distances were measured for each afferent on termination of the experiment by inserting a pin through the RF (marked with ink at the time of recording) and carefully measuring the distance to the DRG along the closest nerve. Afferents were grouped based in their CV (Aβ≥11.2 m/s, Aδ≤11.2≥1.2 m/s and C <1.2 m/s) and subtype (LTMR and HTMR).

2.8. Data analysis

Sample size was determined based on the primary outcome of trajectory of AHTMR needed to create a robust correlation of MT with paw withdrawal threshold (PWT). It was determined that a minimum total sample size of N=62 AHTMR MT would be needed to provide 80% power assuming a two-sided α=0.05 and to detect a correlation of MT with PWT of r=0.35, resulting in at least 12 AHTMRs at each of 5 timepoints including baseline. Prior to analysis, parametric assumptions were evaluated for all variables using histograms and descriptive statistics. Prior to analysis of electrophysiologic variables, we examined the assumption that measurements taken on neurons from the same animal are independent of one another (i.e., that neurons selected randomly across animals are as similar as those from within animals) using the intraclass correlation (ICC). For all measurements, the ICCs <0.22, indicating support for the independence assumption; thus, all analyses were conducted assuming each neuron represented an independent measurement of others taken from the same animal. Data are presented as appropriate to their underlying distributions with mean and standard deviation for normally distributed data, and median and range for non-parametric data. For behavioral withdrawal analysis of PWT a linear mixed-effects model was used to account for the repeated measures within each animal. Because animals were sacrificed according to a randomly generated schedule at 2, 4, 8, and 12 weeks, there were missing values associated with the week of sacrifice. The PWT was regressed on to time (week after injury), group, and a random intercept for each animal was determined. The curvilinear nature of the change trajectory was modeled using a quadratic term ($time^2$). The impact of group on change trajectories was assessed using a likelihood ratio test. Predictions from the model and their confidence intervals were generated using simulations from the model assuming an animal with a median intercept. The correlation of MT over time was done using Spearman correlation, as well as the correlation of MT and PWT. Differences between cell population proportions in the sham and pSNL groups were examined using Chi-square. For cellular data standard parametric (Student’s t-test, one-way ANOVA, linear regression) or nonparametric (Mann-Whitney U-test, Kruskall-Wallis) tests were used, depending on normality. Statistical tests were carried out using multiple packages (R version 3.3.2; OriginPro 7.5, Northampton, MA; InStat/Prism, Graph Pad Software, San Diego, CA).

3. Results

3.1 Effects of L5 pSNL on impaled L4 DRG cell distribution

This study included 302 cells recorded in a stable fashion from the L4 dorsal root ganglion ipsilateral to pSNL or sham surgery (Fig. 1 A and B). Of these, 50 cells were from sham and 252 cells from L5 pSNL animals. Summaries of all findings in neurons and behavior as a result of injury and during resolution of the injury are presented in Table 1. As previously noted, cells from all sham animals were studied 2 weeks after surgery whereas cells after L5 pSNL were studied at 2, 4, 8, and 12 weeks after surgery. Although the pSNL groups contained cells in all three categories (P-RF, N-RF and unexcitable), the sham group had no N-RF cell.

Cells were classified as positive receptive field detected (P-RF), not excitable (UNEX), or no receptive field detected (N-RF). Cells from sham animals that had P-RF were classified as: (LTMR [n=20; 12 hair; 8 RA], 5 muscle spindle (MS)], and HTMR [n=20; 15 AHTMR; 5 CHTMR]). For sham animal cells with N-RF, only S-type cells were found (n=5) and no F-type or UNEX cells were found. After L5 pSNL, overall more cells were found that had N-RF ($p<0.001$). This difference from sham remained until 12 weeks after injury when the distribution was no different from sham. Thus, the likelihood of impaling cells which met passive membrane property definitions, but which were not excitable (UNEX) was increased in recordings from animals after pSNL as was the likelihood of impaling cells that were excitable, but for which a mechanical RF could not be identified (N-RF). After pSNL cells (n=252) found were classified as follows: **Week 2 (W2):** n=58; *40 N-RF* [15 F-type; 10 S-type; 15 UNEX] and *18 P-RF* [5 LTMR (3 Hair; 1 RA; 1 MC), 13 HTMR (13 AHTMR and 0 CHTMR), and 0 MS)]. **Week 4 (W4):** n=77; *40N-RF* [20F-type; 12S-type; 8UNEX] and *37 P-RF* [17/37 LTMR (9 Hair; 8 RA; 0 MC), 15 HTMR (14 AHTMR and 1 CHTMR) and 5 MS]. **Week 8 (W8):** n=63; *18 N-RF* [7 F-type, 8 S-type, 3 UNEX] and *45 P-RF* [20 LTMR (12 Hair, 8 RA, 0 MC), 14 HTMR (12 AHTMR and 2 CHTMR) and 11 MS]. **Weeks 12 (W12):** n=54; *12 N-RF* (5 F-type; 4 S-type; 3 UNEX) and *42 P-RF* [20 LTMR (9 Hair, 11 RA, 0 MC), 16 HTMR (13 AHTMR and 3 CHTMR) and 6 MS].

The distribution of cells recorded and analyzed by group in the study is diagrammed in Fig. 2A. In sham animals few neurons had no receptive fields (N-RF), and only S-types were found (no UNEX or F-types). The electrophysiological data obtained demonstrated a significant difference in distribution of N-RF and P-RF cells ($p<0.001$). The distribution was significantly different at 2 weeks after pSNL compared to control and remained different through 8 weeks ($p=0.02$), but was not different from control at 12 weeks after pSNL ($p=0.09$). A larger percentage of N-RF and UNEX was present at 2 weeks after injury than P-RF afferents (69% [N-RF and UNEX] versus 31% [P-RF]) compared to week 12 after injury (34% [N-RF and UNEX] vs 66% [P-RF]). This inversion of the cellular distribution was reached in a gradual, time dependent manner (Fig. 2A) and greatly depends on the LTMR (W2: 5/58, 9% vs W12:20/53, 38%) and MS (W2: 0/58, 0% vs W12: 6/39, 11%) groups availability rather than HTMR (AHTMR [W2: 13/58, 22% vs W12: 15/53, 25%] and CHTMR [W2; 0/58, 0% vs W12: 3/54, 6%]). N-RF and MS and CHTMR cell recordings were not analyzed further, except CHTMR for CV for comparison with other cells.

Summary/interpretation: Partial-SNL injury results in changes in distribution of fast conducting neurons and the character of their responses that resolve over time. The distribution change after injury largely results from neurons that cannot be activated. The inability to activate these subpopulations of neurons may create an altered state that modulates the perception of mechanical stimulation after injury

3.2 Effects of pSNL on DRG cell mechanical threshold (MT) and Paw Withdrawal Threshold (PWT)

L5 pSNL animals were randomly assigned at various time points to electrophysiologic analysis. No association between baseline thresholds and randomized assignment was found supporting the performance of the randomization. L5 pSNL induced a significant ($p<0.001$) sensitization of fast conducting mechano nociceptors (AHTMR sham: median 147 mN [range: 13.7 to 980 mN] vs AHTMR W2: median 5.9 mN [range: 0.08 to 80]) and the desensitization of tactile L4 afferents (LTMR sham: median 0.13 mN [range: 0.08 to 1.57 mN] vs LTMR W2: median 2.8 mN [range: 0.4 to 3.9 mN]). As shown in Fig. 2B, these changes in afferent sensibility began to rapidly reverse towards normal (W4, increasing thresholds in AHTMR and decreasing thresholds in LTMR) and become significant 8 weeks (W8) after the L5 pSNL compared to 2 weeks ($p<0.05$, AHTMR W8: median 89 mN [range: 13.7 to 588 mN]; $p<0.01$ LTMR W8: median 0.2 mN [range: 0.08 to 3.9 mN]). Slow conducting mechano nociceptors (CHTMR) were detectable in sham (n=5, median: 980 mN [range 588 to 980 mN]) and weeks 4 (n=1, 98 mN), 8 (n=2, median: 495 mN [range: 9.8 to 980 mN] and 12 (n=3, median: 784 mN [range: 588 to 980 mN), but not at week 2. No further analysis was performed on these afferents (CHTMR).

Paw withdrawal threshold (PWT) at baseline was 21.9±6.8 g. Following L5 pSNL, the PWT dropped significantly ($p<0.001$), reaching a low of 4.7±3.7 g at the 2 week timepoint and then gradually recovered to no different from baseline by 13 weeks after injury (16.6±10.4 g). The trajectory of the PWT recovery was nonlinear with a significant difference between the change trajectories between the sham and pSNL groups (X^2 (3) = 68.0, $p < 0.0001$) (Fig. 3). Sham animal PWT was different from the pSNL group (did not change over time which was different from the pSNL animals ($p<0.001$). Modeling of the AHTMR and LTMR curves over time using linear, nonlinear and categorical analysis found the quadratic to provide the best fit for both (AHTMR: R2 = 0.50 vs R2 = 0.56, p = 0.017; LTMR: R2 = 0.33 vs R2 = 0.37, p = 0.036). However, the correlations with PWT were opposite in direction (Fig. 4 A and B). There was a negative correlation between LTMR MT and PWT with LTMR MT desensitizing (increasing thresholds) with sensitization (decreased PWT) (Spearman non-parametric correlation, r = −0.32, p = 0.012). At the same time there was a positive correlation between the AHTMR MT and the PWT with the AHTMR sensitizing (decreasing thresholds) with sensitization (decreasing PWT thresholds) (Spearman non-parametric correlation, r = 0.35, p = 0.011). The correlations for AHTMR MT and LTMR MT with PWT also followed a non-linear pattern when compared to the AHTMR MT to PWT (Fig. 4, blue lines). There was a significant negative correlation of the AHTMR and the LTMR (Spearman non-parametric correlation, r = −0.41, p = 0.009).

Summary/interpretation: Of the responsive neurons after p-SNL injury the AHTMR are sensitized and the LTMR are desensitized and these changes are correlated to the paw withdrawal threshold. This indicates that the behavioral response can be explained by the AHTMR sensitization as the main nociceptive information carrier after injury and not the remaining active tactile afferents.

3.3. Effects of L5 pSNL on the L4 DRG cells active and passive electrical properties

Active Properties

3.3.1. AP Amplitude—Normal (sham) fast conducting nociceptive afferents showed a significantly ($p<0.001$) greater AP amplitude (AHTMR: 64±1.2 mV) compared to tactile afferents (LTMR: 43±1.8 mV). This modality specific AP amplitude differential between afferents subtypes was upheld at all timepoints but W8. As shown in Fig. 5 (A, C and D), W2 after L5 pSNL, the AP amplitude of both types of afferents was significantly reduced (AHTMR: $p<0.001$ and $p<0.01$ LTMR) (AHTMR: 51±3.1 mV and LTMR: 30±0.2 mV). Although tactile afferents rapidly recover (W4: $p<0.05$, 40±2.5 mV), in both cases the afferent AP amplitudes were not different from normal by W12 (AHTMR: 59±3 mV and LTMR: 37±2 mV).

3.3.2. AP duration (D50)—The normal (sham) AP duration was significantly ($p<0.001$) different between fast conducting nociceptive (AHTMR: 1.5±0.09 ms) and tactile afferents (LTMR: 0.7±0.03 ms). This modality specific differential of the AP duration was upheld at all timepoints after L5 pSNL (LTMR>1ms<AHTMR). As shown in Fig. 5 (B and C), two weeks after injury (W2) tactile afferents showed a significant increase in the AP duration (D50) (W2 LTMR D50: 0.8±0.05 ms) that only recovers ($p<0.05$) by week 12 (W12 LTMR D50: 0.6±0.04 ms).

3.3.3. AHP amplitude—Two weeks after L5 pSNL a significant ($p<0.05$) reduction of the AHP amplitude of both afferents was observed ($p<0.05$, AHTMR sham: 12±1 mV vs. W2 AHTMR: 8±1 mV; $p<0.001$, LTMR sham: 9±0.7 mV vs W2: 4±0.6 mV) (Fig. 5 (C, D and E). This simultaneous but uneven (in magnitude between afferents) reduction in the AHP amplitude, induced a significant ($p<0.05$) difference between nociceptive and tactile afferents AHP amplitude, not previously observed in sham animals. A rapid recovery of the AHP amplitude of tactile afferents (W4 LTMR AHP amplitude: 8±0.6 mV) eliminated this differential with fast conducting nociceptors, although the AHTMR did not fully recover until W12 (W12 AHTMR: 14±1 mV, $p<0.01$) (Fig. 5E).

3.3.4. AHP duration (AHP50)—Normal (sham) fast conducting nociceptive (AHTMR: 13.8±1.6 ms) afferents showed a significantly ($p<0.001$) greater AHP50 than tactile (LTMR: 4.7±0.5 ms) afferents. This modality specific AHP duration differential between afferents subtypes was eliminated by W2 after L5 pSNL by the significant ($p<0.01$) reduction in the AHP50 of fast conducting nociceptive afferents (W2 AHTMR AHP50: 6.7±1.3 ms) and did not recover by 12 weeks (W12) after nerve damage (Fig. 5C, D and F).

Passive Properties

3.3.5. Membrane potential (Em, mV)—L5 pSNL induced the steady membrane depolarization of both types of mechano-sensitive afferents along all studied time points (W2-W12) (Fig. 6A). Although this L5 pSNL-induced depolarization process only became statistically significant for both afferents at W8 (AHTMR: $p<0.05$ [r^2: 0.84] and LTMR: $p<0.001$ [r^2: 0.96]), its effects had a differential initial effect with respect to the afferent modality. At W2, the membrane depolarization had a greater effect on fast conducting nociceptors (AHTMR: Sham: −62.7±1.7 mV to W2: −56.5±2.2 mV) than tactile afferents (LTMR: Sham: −66.3±1.6 mV to W2: −65.2±3.2 mV). This differential effect renders the Em of both afferents significantly ($p<0.05$) different at W2 but this difference rapidly dissipated as a consequence of an increased depolarization of the tactile afferents in following weeks (W4-W12) (Fig. 6A).

3.3.6. Input resistance (Ri, MΩ).—In sham animals, nociceptive afferents showed a significantly ($p<0.01$) higher Ri than tactile afferents (AHTMR: 162±20 MΩ vs LTMR: 110±10 MΩ). This difference rapidly disappeared after nerve injury (W2), affecting both types of afferents. Although both types of afferents showed a reduction in Ri, it only became significant ($p<0.05$) in nociceptors at W8, prior to recovery in W12. However, we also observed that despite the full recovery of nociceptors ($p<0.05$), tactile afferents continued to demonstrate an incremental increase in Ri from W4 to W12. (Fig. 6B).

3.3.7. Time constant (τ, ms).—L5 pSNL induced a transient decrease in duration of τ in both types of afferents (Fig. 6C). This decrease became significant ($p<0.05$) at W4 for tactile afferents (LTMR Sham: 2.7±0.4 ms vs LTMR W4: 1.7±0.4 ms) and at W8 for fast conducting nociceptors (AHTMR sham: 3.3±0.3 vs AHTMR W8: 2±0.2 ms), but it recovered to sham values at W12 ($p<0.05$, LTMR).

3.3.8. Capacitance (Cm, pF)—Overall the Ri and τ changes in both types of afferents result in a steady, but non-significant, decrease of the membrane capacitance (Cm). Only LTMR Cm, as shown in Fig. 6D, experienced a transient (W8) significant ($p<0.05$) increase in the Cm compared to AHTMR afferents at the same time point (LTMR W8: 27±3 pF vs AHTMR W8: 19±3 pF).

3.3.9. CV vs L4 cellular subtype after L5 pSNL—Although afferents with a wide range of CV were collected at all timepoints, the number and specific CV range were significantly different between time points. CV of tactile afferents from sham animals were significantly ($p<0.001$) faster (Aβ and Aδ ranges only) than nociceptive afferents (LTMR sham: 14.2±1.7 m/s [Aβ: median 21.6 m/s [range 14.5 to 35]; Aδ: median 7.5 m/s [range: 1.5 to 11.2 m/s] vs AHTMR sham: 5.1±0.9 m/s [Aβ: median 12.2 m/s [range 12 to 12.3 m/s]; Aδ median: 5.7 m/s [range 1.5 to 10.4 m/s]). However, 2 weeks after L5 pSNL the composition of detectable afferents in both modalities are significantly ($p<0.05$) biased towards specific CV ranges. As show in Fig. 7A at W2, recorded tactile afferents were restricted to the Aβ range but significantly ($p<0.05$) restricted to slow CV within this range (Aβ LTMR sham: 22 m/s [range 15 to 35 m/s] vs Aβ LTMR W2: 14 m/s [range: 11.3 to 18.6 m/s]). This transient change in the composition of mechanically sensitive afferents recovered

at W4 ($p<0.05$, tactile) (Aβ LTMR W4: median 22 m/s [range: 13 to 31 m/s]; Aδ LTMR W4: median 5 m/s [range: 3.5 to 7.9 m/s]) and W12 ($p<0.05$, nociceptive) (Aβ AHTMR W12: median 16.8 m/s [range 14.8–18.8 m/s]; Aδ AHTMR W12: median 4.2 m/s [range 1.7 to 10.9 m/s]).

3.3.10 CV vs AP duration (D50) after L5 pSNL—In sham animals a correlation between CV and AP duration (D50) was found between neurons, both in the LTMR and AHTMR neuron groups. Faster conducting fibers corresponded to somas with shorter APs (LTMR: $r^2 = -0.45$, $p<0.01$ and HTMR: $r^2=-0.24$, $p<0.05$) (Fig. 7B). While this relationship was upheld for LTMR at all timepoints (W2-W12), at W2 AHTMR showed a significant inversion of this correlation as cells with faster conducting fibers show longer APs ($r^2=0.53$, $p<0.01$). This inversion on the CV/AP duration correlation was transient (W2 only) and recovered in following time points (W4-W12).

Summary/interpretation: Partial-SNL injury results in the transient modulation of somatic electrical properties in both LTMR and AHTMR mechanoreceptors. Overall, these changes reflect an increase in electrical excitability in nociceptive afferents (e.g. greater neuronal activity) and a widespread disruption in baseline electrical stability (e.g. altered Em) for both LTMR and AHTMR afferents. Some of these changes do not completely revert to normal after behavioral recovery indicating the history-dependent, additive electrical effects of injury on these afferents membranes.

4. Discussion

This report addresses two fundamental aspects of tactile hypersensitivity after nerve injury and during recovery: the identity of primary sensory afferent subtype changes from injury and the reliance of behavioral hypersensitivity on abnormal peripheral signaling over time during resolution. These results corroborate previous work [4] which showed opposing actions of nerve injury on tactile afferents (LTMRs) and nociceptive afferents (HTMRs) which are desensitized and sensitized, respectively. This result argues against a primary role of sensitized LTMRs in hypersensitivity. On the contrary, LTMR desensitization may contribute to behavioral hypersensitivity indirectly. The strong relationship between the time courses of recovery of tactile and nociceptive afferents and of resolution from hypersensitivity, although alone not proving causality, suggests strongly that behavioral hypersensitivity in this surgical model requires both abnormal tactile and nociceptive peripheral input.

Peripheral nerve injury affects thresholds of specific fibers and also electrical excitability of dorsal root ganglion cells from mechanical activation within their receptive fields. In pSNL animals the likelihood of finding cells with N-RF or UNEX is increased relative to sham. These are cells that both have no detectable receptive field, one electrically excitable (N-RF) and the other unable to be depolarized (UNEX). The increase in “silent” cell numbers following injury is interesting, and may represent an injured phenotype that cannot transmit information effectively. The reduced input from these cells may alter integration of input from remaining cells, potentially leading to increased behavioral response to activation. Consistent with these notions is that “silent” cells tend to disappear as the resolution of the

injury progresses over time approaching the sham distribution. It is also possible that the UNEX cells represent non neuronal cells, although the membrane potential is greater than would be expected from a glia cell. There may also be an artifactual increase in the probability of impaling neurons resulting from injury induced changes in cellular morphology or volume [24; 41]. Further studies to definitively identify the “silent” cells using simultaneous staining and electrophysiologic identification will be informative to understand the nature of these cell populations.

The electrical properties of both AHTMR and LTMR neurons are extensively changed by injury [15; 29; 31]. Baseline resting membrane potential (Em) is more negative in LTMR compared to AHTMR while initially after injury the AHTMR Em depolarizes while the LTMR Em does not. Following injury the changes occur in concert with a similar slope in changes over time. However, the reason is likely different; LTMR trying to increase information due to failing conduction and AHTMR increasing activity due to injury and sensitization. Simultaneously resistance decreases as the rheobase changes likely reflecting effects of inflammation and cellular changes from injury [18; 24; 41]. Changes in sodium channel expression may alter excitability, but other channels may play a role and be targets for intervention [2; 33; 36]. Interestingly, despite the resolution of behavior and some electrical changes over time, many altered electrical properties persist and may suggest a vulnerable period between resolution of behavior and normalization of neuronal electrical activity. Understanding how these long lasting changes in the electrical properties of AHTMR and LTMR afferents are integrated at the spinal level may be important for understanding their individual or combined roles in resolution of pain at a behavioral level.

Sensitization of AHTMRs in creating a nociceptive signal after injury is well accepted in nerve injury, incisional models, and inflammatory models of pain [16; 18; 31]. However, LTMR desensitization from injury has not been reported until recently. This likely relates to technologic difficulties in assessing LTMR sensibility and through assuring the lack of injury effect in sham or naïve animals during electrophysiologic recording [16; 18; 31; 44]. MT in LTMRs from sham animals in previous studies is similar our pSNL injured animals, possibly reflecting injury from the recording preparation. [44]. Other technical nuances may contribute including differences in temperature, whether *in vivo* and/or *in situ*, and disruption of proximal and distal connections. Washout of inflammatory mediators around the DRG with artificial CSF perfusion in our studies compared to paraffin which traps these molecules and provides for their build up in proximity to the cell bodies and axons could also contribute. These technical difficulties make assessment of normal LTMR sensibility very difficult requiring extensive assurance to maintain temperature, assure the lack of inflammatory mediator building, and a limited search paradigm that reduces peripheral sensitization, or in the case of LTMR, desensitization process. One of the unique findings in all of our studies is the lack of spontaneous activity in A-fibers. A-fiber mediated spontaneous activity could reflect injury during the preparation and may not be a result of nerve injury itself [29; 31; 44]. This acute injury is another reason that LTMR desensitization has not been reported as the baseline encountered is desensitization from the acute injurious effects of the prep, nerve injury or denervation, and inflammation masking changes from nerve injury.

The loss of LTMR sensibility is of interest in that the same injury produces a significant decrease in threshold in one fiber type and significant increase in the other. This underscores the differences in the two nerve fiber types that are poorly understood. Nevertheless, LTMR desensitization in perception of nociceptive information and ultimately pain is not novel [26; 30; 34]. Loss of fiber function may be associated with pain, but many examples exist where this does not routinely occur [17; 35; 40]. Additionally, tactile input has been cast as a driver for nociception in the chronic states where allodynia is present [13; 28]. At the same time, tactile inputs have also been reported to have important inhibitory effects on nociceptive throughput in the dorsal horn thus affecting central processing and pain perception [21; 32]. LTMR are activated by vibratory stimuli over a discrete frequency range within their receptive field and this is used to distinguish LTMRs from AHTMRs, particularly following injury [4; 8; 9]. Activating LTMR via vibration produces a shift in perceived pain perception of noxious stimuli and is likely the fundamental effect of transcutaneous nerve stimulation used for pain relief [30]. The mechanism of this modulatory effect on noxious input is unclear, but could be peripheral, cortical, the dorsal horn of the spinal cord, or a combination of these locations [23; 38]. Thus activation of LTMRs and resulting modulation of perception from other neurons may be valuable to recovering normal sensibility and pain free function.

Peripheral LTMR desensitization appears to part of the injury process and as such may play a role in perception of the noxious stimuli acutely and over time until resolution of injury. This role of LTMRs in pain signaling, at least acute pain signaling, has been validated recently using advanced optogenetic approach and suggests that pain from A-fiber nociceptors is alleviated with concurrent activation of LTMRs [1]. Just like selective activation of LTMR does not cause pain, selective deactivation does not cause pain and the response may be related to integration of other inputs [25]. Furthermore the mechanically sensitive neurons are likely to respond to more than mechanical stimuli rendering input and activity in the dorsal horn modulated by other modalities simultaneously [3]. Thus, loss of large fiber input is not sufficient to cause pain, but may be a modulator or even act as an accelerator of other noxious inputs. This furthers the notion that neural activity in different sensory neuron subpopulations is important to the perception of pain and further suggests that the most effective pain treatment regimens will require altering input in various neuronal subpopulations simultaneously or at least in a deliberate and targeted fashion.

Limitations of this investigation are the focus on fast conducting afferents and their response to mechanical activation. Slow conducting C-high threshold mechanoreceptors were found incidentally, but we did not study C-fibers and made no conclusions based on the limited number. Further study of C-fiber changes would more completely delineate changes of afferent inputs, as they play a role in nociception as well. Additionally, the reliance solely on mechanical activation without incorporation of non-reflexive behavioral pain measures is also a limitation and further studies to understand the role of fast conducting afferent subsets in non-reflexive behaviors will be important to more completely understanding the implications of their inputs.

These data highlight and validate the rapid injury-induced sensitization and desensitization process that occurs in different subtypes of mechano-sensitive peripheral sensory neurons.

There is likely a pivotal role for the change in specific subpopulations of mechanosensitive neurons during the resolution of injury induced pain behavior that underlies the animals' recovery pattern. Likely the full recovery of the behavior requires the normalization of both types of alterations in mechanical sensibility. The incomplete resolution of specific changes in electrical properties with the normalization of behaviors and the neural input alterations point to the complexity of successfully addressing effective management for nerve injury induced pain. We speculate that these persistent electrical changes and excitation changes in the peripheral neurons after apparent resolution of behavioral hypersensitivity may result in an underlying vulnerability to subsequent injury that could result in disruption of resolution and predispose to persistent or chronic pain states.

Acknowledgments

Research Support

Funding provided by the National Institutes of Health through grants NS074357 (TJM), GM113852 (TJM, MDB, DGR, JCE), and GM104249 (DGR, TJM).

References

[1]. Arcourt A, Gorham L, Dhandapani R, Prato V, Taberner FJ, Wende H, Gangadharan V, Birchmeier C, Heppenstall PA, Lechner SG. Touch Receptor-Derived Sensory Information Alleviates Acute Pain Signaling and Fine-Tunes Nociceptive Reflex Coordination. Neuron 2017;93(1):179–193. [PubMed: 27989460]

[2]. Bennett DL, Clark AJ, Huang J, Waxman SG, Dib-Hajj SD. The Role of Voltage-Gated Sodium Channels in Pain Signaling. Physiol Rev 2019;99(2):1079–1151. [PubMed: 30672368]

[3]. Boada MD, Eisenach JC, Ririe DG. Mechanical sensibility of nociceptive and non-nociceptive fast-conducting afferents is modulated by skin temperature. J Neurophysiol 2016;115(1):546–553. [PubMed: 26581873]

[4]. Boada MD, Gutierrez S, Aschenbrenner CA, Houle TT, Hayashida K, Ririe DG, Eisenach JC. Nerve injury induces a new profile of tactile and mechanical nociceptor input from undamaged peripheral afferents. J Neurophysiol 2015;113(1):100–109. [PubMed: 25274350]

[5]. Boada MD, Gutierrez S, Giffear K, Eisenach JC, Ririe DG. Skin incision-induced receptive field responses of mechanosensitive peripheral neurons are developmentally regulated in the rat. J Neurophysiol 2012;108(4):1122–1129. [PubMed: 22673323]

[6]. Boada MD, Gutierrez S, Houle T, Eisenach JC, Ririe DG. Developmental differences in peripheral glabrous skin mechanosensory nerve receptive field and intracellular electrophysiologic properties: phenotypic characterization in infant and juvenile rats. Int J Dev Neurosci 2011;29(8):847–854. [PubMed: 21856407]

[7]. Boada MD, Houle TT, Eisenach JC, Ririe DG. Differing neurophysiologic mechanosensory input from glabrous and hairy skin in juvenile rats. J Neurophysiol 2010;104(6):3568–3575. [PubMed: 20926608]

[8]. Boada MD, Martin TJ, Peters CM, Hayashida K, Harris MH, Houle TT, Boyden ES, Eisenach JC, Ririe DG. Fast-conducting mechanoreceptors contribute to withdrawal behavior in normal and nerve injured rats. Pain 2014;155(12):2646–2655. [PubMed: 25267211]

[9]. Boada MD, Martin TJ, Ririe DG. Nerve injury induced activation of fast-conducting high threshold mechanoreceptors predicts non-reflexive pain related behavior. Neurosci Lett 2016;632:44–49. [PubMed: 27544012]

[10]. Borsook D, Kussman BD, George E, Becerra LR, Burke DW. Surgically induced neuropathic pain: understanding the perioperative process. Ann Surg 2013;257(3):403–412. [PubMed: 23059501]

[11]. Brennan TJ. Pathophysiology of postoperative pain. Pain 2011;152(3 Suppl):S33–40. [PubMed: 21232860]

[12]. Cabanes C, Lopez de Armentia M, Viana F, Belmonte C. Postnatal changes in membrane properties of mice trigeminal ganglion neurons. J Neurophysiol 2002;87(5):2398–2407. [PubMed: 11976377]

[13]. Campbell JN, Raja SN, Meyer RA, Mackinnon SE. Myelinated afferents signal the hyperalgesia associated with nerve injury. Pain 1988;32(1):89–94. [PubMed: 3340426]

[14]. Chaplan SR, Bach FW, Pogrel JW, Chung JM, Yaksh TL. Quantitative assessment of tactile allodynia in the rat paw. J Neurosci Methods 1994;53(1):55–63. [PubMed: 7990513]

[15]. Djouhri L L5 spinal nerve axotomy induces sensitization of cutaneous L4 Abeta-nociceptive dorsal root ganglion neurons in the rat in vivo. Neurosci Lett 2016;624:72–77. [PubMed: 27173166]

[16]. Djouhri L, Fang X, Koutsikou S, Lawson SN. Partial nerve injury induces electrophysiological changes in conducting (uninjured) nociceptive and nonnociceptive DRG neurons: Possible relationships to aspects of peripheral neuropathic pain and paresthesias. Pain 2012;153(9):1824–1836. [PubMed: 22721911]

[17]. Dyck PJ, Lambert EH, O'Brien PC. Pain in peripheral neuropathy related to rate and kind of fiber degeneration. Neurology 1976;26(5):466–471. [PubMed: 177904]

[18]. Eliav E, Benoliel R, Tal M. Inflammation with no axonal damage of the rat saphenous nerve trunk induces ectopic discharge and mechanosensitivity in myelinated axons. Neurosci Lett 2001;311(1):49–52. [PubMed: 11585565]

[19]. Gallego R, Eyzaguirre C. Membrane and action potential characteristics of A and C nodose ganglion cells studied in whole ganglia and in tissue slices. J Neurophysiol 1978;41(5):1217–1232. [PubMed: 702193]

[20]. Gracely RH, Lynch SA, Bennett GJ. Painful neuropathy: altered central processing maintained dynamically by peripheral input. Pain 1992;51(2):175–194. [PubMed: 1484715]

[21]. Green BG, Schoen KL. Evidence that tactile stimulation inhibits nociceptive sensations produced by innocuous contact cooling. Behav Brain Res 2005;162(1):90–98. [PubMed: 15922069]

[22]. Guan Y, Yuan F, Carteret AF, Raja SN. A partial L5 spinal nerve ligation induces a limited prolongation of mechanical allodynia in rats: an efficient model for studying mechanisms of neuropathic pain. Neurosci Lett 2010;471(1):43–47. [PubMed: 20067820]

[23]. Hollins M, McDermott K, Harper D. How does vibration reduce pain? Perception 2014;43(1):70–84. [PubMed: 24689133]

[24]. Igarashi T, Yabuki S, Kikuchi S, Myers RR. Effect of acute nerve root compression on endoneurial fluid pressure and blood flow in rat dorsal root ganglia. J Orthop Res 2005;23(2):420–424. [PubMed: 15734257]

[25]. Ji ZG, Ito S, Honjoh T, Ohta H, Ishizuka T, Fukazawa Y, Yawo H. Light-evoked somatosensory perception of transgenic rats that express channelrhodopsin-2 in dorsal root ganglion cells. PLoS One 2012;7(3):e32699.

[26]. Kakigi R, Shibasaki H. Mechanisms of pain relief by vibration and movement. J Neurol Neurosurg Psychiatry 1992;55(4):282–286. [PubMed: 1583512]

[27]. Koltzenburg M Neural mechanisms of cutaneous nociceptive pain. Clin J Pain 2000;16(3 Suppl):S131–138. [PubMed: 11014457]

[28]. Landerholm AH, Hansson PT. Mechanisms of dynamic mechanical allodynia and dysesthesia in patients with peripheral and central neuropathic pain. Eur J Pain 2011;15(5):498–503. [PubMed: 21094619]

[29]. Liu CN, Wall PD, Ben-Dor E, Michaelis M, Amir R, Devor M. Tactile allodynia in the absence of C-fiber activation: altered firing properties of DRG neurons following spinal nerve injury. Pain 2000;85(3):503–521. [PubMed: 10781925]

[30]. Lundeberg T The pain suppressive effect of vibratory stimulation and transcutaneous electrical nerve stimulation (TENS) as compared to aspirin. Brain Res 1984;294(2):201–209. [PubMed: 6608397]

[31]. Ma C, Shu Y, Zheng Z, Chen Y, Yao H, Greenquist KW, White FA, LaMotte RH. Similar electrophysiological changes in axotomized and neighboring intact dorsal root ganglion neurons. J Neurophysiol 2003;89(3):1588–1602. [PubMed: 12612024]

[32]. Narikawa K, Furue H, Kumamoto E, Yoshimura M. In vivo patch-clamp analysis of IPSCs evoked in rat substantia gelatinosa neurons by cutaneous mechanical stimulation. J Neurophysiol 2000;84(4):2171–2174. [PubMed: 11024105]

[33]. Nonaka T, Honmou O, Sakai J, Hashi K, Kocsis JD. Excitability changes of dorsal root axons following nerve injury: implications for injury-induced changes in axonal Na(+) channels. Brain Res 2000;859(2):280–285. [PubMed: 10719075]

[34]. Ottoson D, Ekblom A, Hansson P. Vibratory stimulation for the relief of pain of dental origin. Pain 1981;10(1):37–45. [PubMed: 7232010]

[35]. Periquet MI, Novak V, Collins MP, Nagaraja HN, Erdem S, Nash SM, Freimer ML, Sahenk Z, Kissel JT, Mendell JR. Painful sensory neuropathy: prospective evaluation using skin biopsy. Neurology 1999;53(8):1641–1647. [PubMed: 10563606]

[36]. Rahman W, Dickenson AH. Voltage gated sodium and calcium channel blockers for the treatment of chronic inflammatory pain. Neurosci Lett 2013;557 Pt A:19–26.

[37]. Rossaint J, Zarbock A. Perioperative Inflammation and Its Modulation by Anesthetics. Anesth Analg 2018;126(3):1058–1067. [PubMed: 28922235]

[38]. Salter MW, Henry JL. Evidence that adenosine mediates the depression of spinal dorsal horn neurons induced by peripheral vibration in the cat. Neuroscience 1987;22(2):631–650. [PubMed: 3670602]

[39]. Sheen K, Chung JM. Signs of neuropathic pain depend on signals from injured nerve fibers in a rat model. Brain Res 1993;610(1):62–68. [PubMed: 8518931]

[40]. Thomas PK. The anatomical substratum of pain evidence derived from morphometric studies on peripheral nerve. Can J Neurol Sci 1974;1(2):92–97. [PubMed: 4140016]

[41]. Tsuyoshi H, Zenzai K, Okado H, Endo N, Shibata M, Hirano S. Sprouting of sensory neurons in dorsal root ganglia after transection of peripheral nerves. Arch Histol Cytol 2006;69(3):173–179. [PubMed: 17031023]

[42]. Woolf CJ. Central sensitization: implications for the diagnosis and treatment of pain. Pain 2011;152(3 Suppl):S2–15. [PubMed: 20961685]

[43]. Yoshida S, Matsuda Y. Studies on sensory neurons of the mouse with intracellular-recording and horseradish peroxidase-injection techniques. J Neurophysiol 1979;42(4):1134–1145. [PubMed: 479922]

[44]. Zhu YF, Henry JL. Excitability of Abeta sensory neurons is altered in an animal model of peripheral neuropathy. BMC Neurosci 2012;13:15. [PubMed: 22289651]

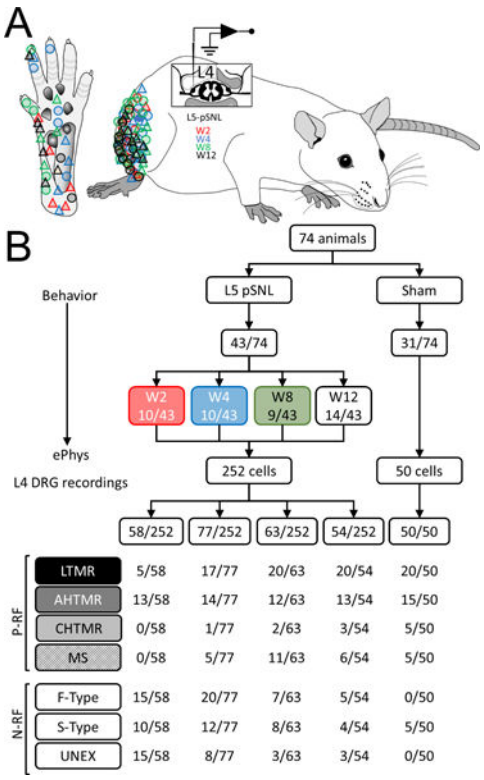

Figure 1.

A. Schematic diagram of the *in vivo* ePhys rat L4 preparation (lateral view) after pSNL in L5. Diagram of lateral flank illustrates the areas where the neuronal receptive field (RF) of the studied afferents were found in hairy skin and glabrous skin (Circles: tactile; Triangles: nociceptors) over time (red: week 2; blue: week 4; green: week 8 and black: week 12). **B.** Flowchart of animals studied and classification of the neurons included in the study per week (W): with mechanical RF (P-RF): low threshold mechanoreceptors (LTMR, black), high threshold mechanoreceptor with A fibers (AHTMR, dark gray), high threshold mechanoreceptor with C fibers (CHTMR, light gray) muscular spindle (MS) and without RF (N-RF): fast AP dynamic mechanically unresponsive (F-type), slow AP dynamics mechanically unresponsive (S-type), unresponsive (mechanically and electrically) (UNEX).

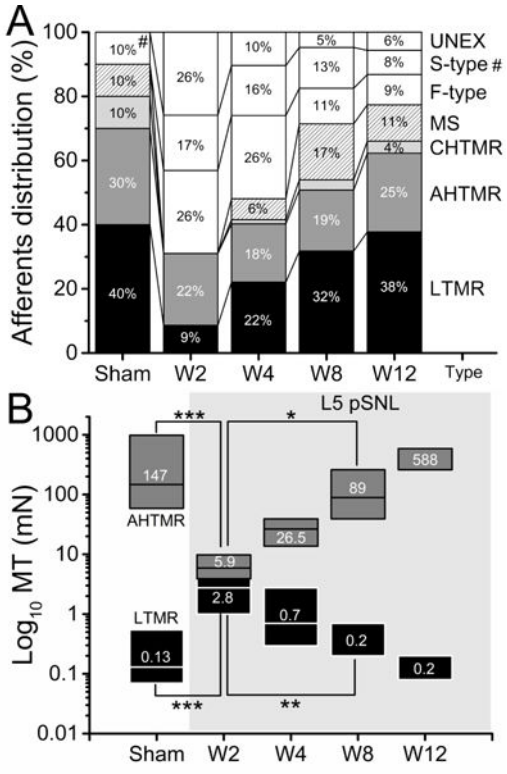

Figure 2.

A. Effect of L5-pSNL in the L4 percent distribution of mechanically sensitive (LTMR, AHTMR, CHTMR and MS) and insensitive (F-type, S-type and UNEX) afferents over time (weeks: W) after L5-pSNL (#: S-type). There is a significant difference in distribution of N-RF and P-RF cells ($p<0.001$). The distribution is significantly different at 2 weeks after pSNL compared to control and remains different through 8 weeks ($p=0.02$), but is no different from control at 12 weeks after pSNL ($p=0.09$). **B.** Effects of the L5-pSNL in the mechanical sensitivity of L4 afferents over time (W). Numbers indicate medians (on top), with boxes representing the 25 and 75 percentiles. LTMR: low-threshold mechanoreceptor and AHTMR: A-fiber high-threshold mechanoreceptor. (*=$p<0.05$; **=$p<0.01$; ***=$p<0.001$).

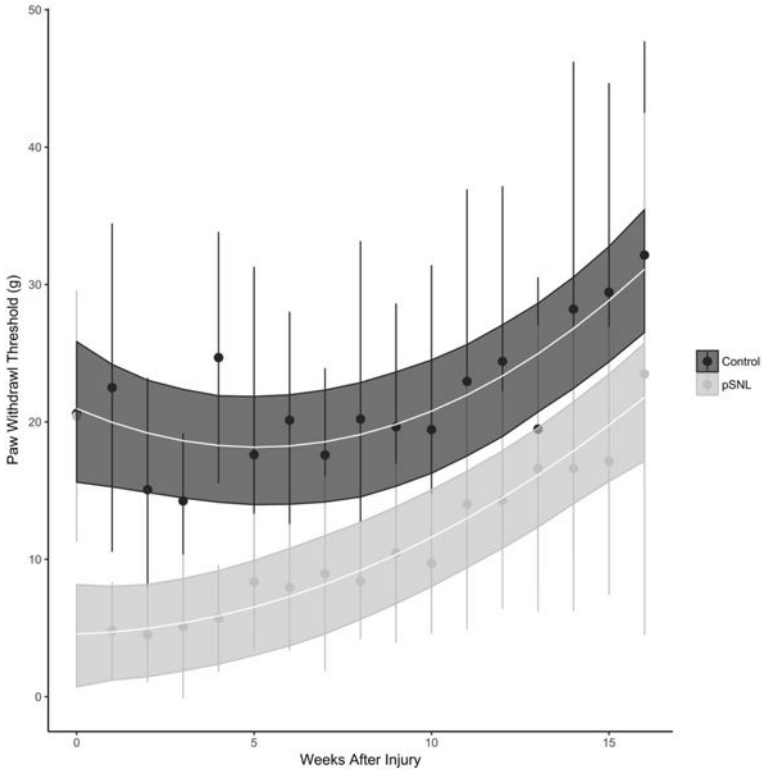

Figure 3.

Trajectory of L5-pSNL on paw withdrawal threshold (PWT) over time. The trajectory of the PWT recovery is nonlinear with a significant difference for the change trajectories between the sham and pSNL groups ($p < 0.0001$). Both sham and pSNL groups have a PWT that is not different at baseline. After the pSNL there is an immediate decrease in PWT (*, $p<0.001$). The difference in PWT persists through 13 weeks after the injury.

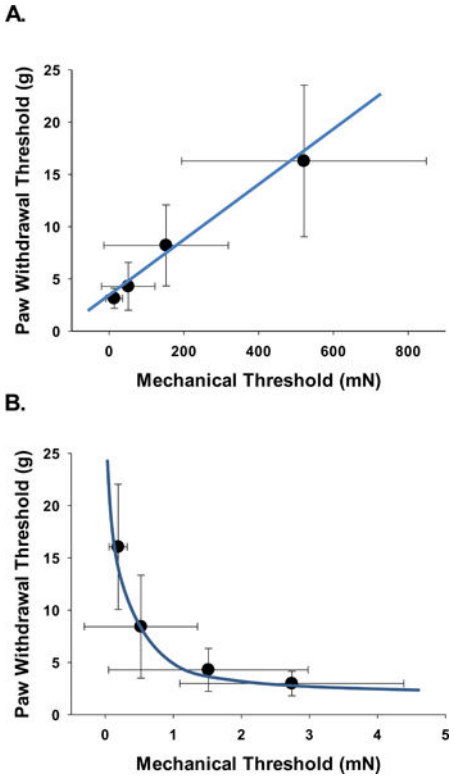

Figure 4.

Correlation of single neuronal mechanical thresholds (MT) and behavior paw withdrawal thresholds (PWT). There is a negative correlation between LTMR MT and PWT with LTMR MT desensitizing (increasing thresholds) with sensitization (decreased PWT) (Spearman non-parametric correlation, $r = -0.32$, $p = 0.012$). At the same time there is a positive correlation between the AHTMR MT and the PWT with the AHTMR sensitizing (decreasing thresholds) with sensitization (decreasing PWT) (Spearman non-parametric correlation, $r = 0.35$, $p = 0.011$). The correlations for AHTMR MT and LTMR MT with PWT follow a non-linear pattern when compared to the AHTMR MT to PWT (blue lines).

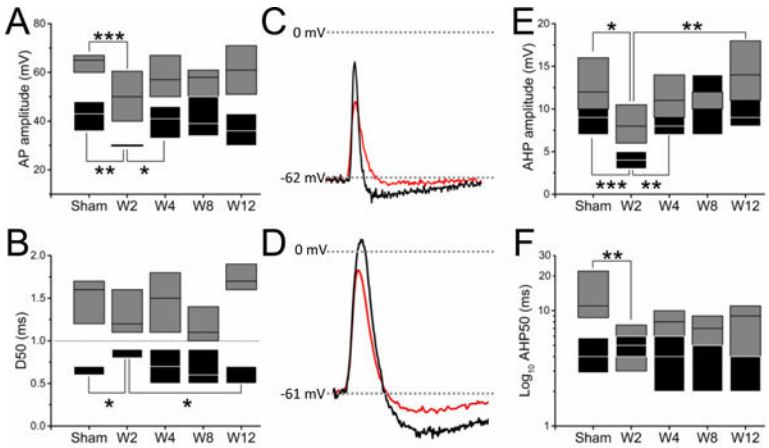

Figure 5.

Effect of L5-pSNL in the L4 mechanosensitive afferent active electrical signature of evoked action potentials over time in weeks (W): spike (**(A)** amplitude [AP amplitude] and **(B)** duration [AP duration; D50]) and AHP: (**(E)** amplitude and **(F)** duration [AHP50]). Representative traces of these effects are presented (black sham and red W2) in tactile **(C)** and nociceptive **(D)** afferents that demonstrate the changes after injury. Boxes represents 25 and 75 percentiles (black: LTMR; gray: AHTMR). (*=p<0.05; **=p<0.01; ***=p<0.001).

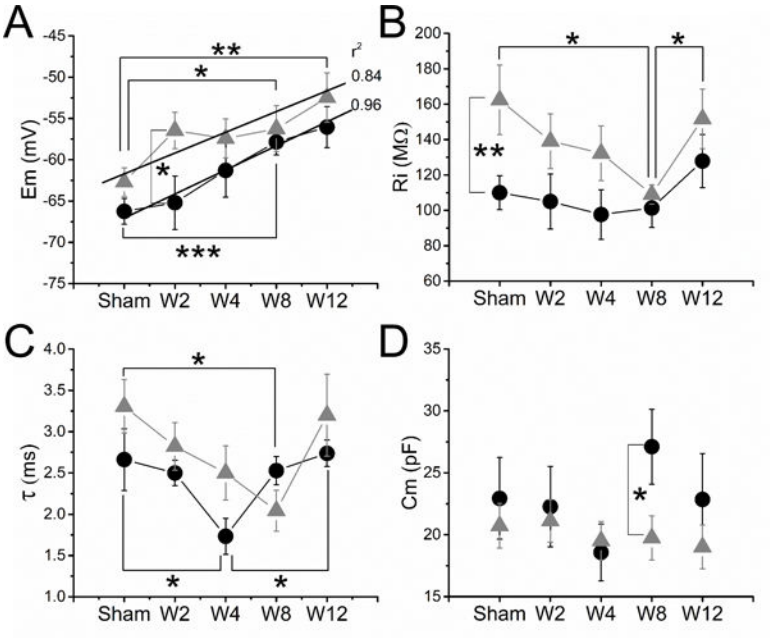

Figure 6.

Effect of L5-pSNL in the L4 mechanosensitive afferents passive electrical properties over time in weeks (W): **(A)** membrane potential (Em), **(B)** input resistance (Ri), **(C)** time constant (**τ**) and **(D)** membrane capacitance (Cm). Data are medians ± SE. Regression lines and r^2 values are shown for Em in LTMRs (black circles) and AHTMR (gray triangles) (*=p<0.05; **=p<0.01; ***=p<0.001).

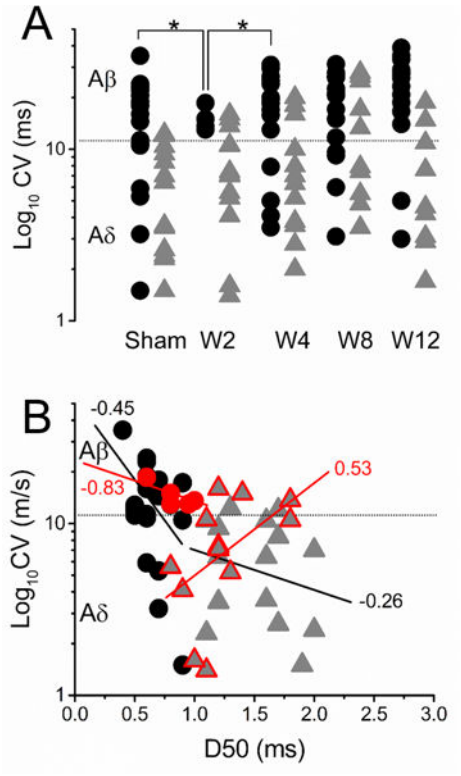

Figure 7.

A. Effect of L5-pSNL in the L4 mechanosensitive afferents CV (black circles: LTMR and gray triangles: AHTMR) over time and **B.** its effects on the relationship between CV and the spike duration (D50) (linear regression and r^2 values) two weeks after injury (red circles: LTMR and red triangles: AHTMR). *=p<0.05.

Table 1.

Summary changes with injury and recovery

Outcome Measure	Injury	Recovery
PWT	↓	↑
AHTMR Threshold	↓	↑
LTMR Threshold	↑	↓
Cells Character:		
N-RF	↑	↓
P-RF	↓	↑
UNEX	↑	↓
Cell Type Distribution:		
AHTMR	NC	NC
LTMR	↓	↑
CHTMR	↓	↑
MS	↓	↑
F-type	↑	↓
S-type	↑	↓
Active Electrical Properties AHTMR:		
AP Amplitude	↓	↑
AP Duration	NC	NC
AHP Amplitude	↓	↑
AHP50	↓	↑
Active Electrical Properties LTMR:		
AP Amplitude	↓	↑
AP Duration	↑	↓
AHP Amplitude	↓	↓
AHP50	NC	NC
Passive Electrical Properties AHTMR:		
Em (mV)	↑	↑
Ri (MΩ)	↓	↓
τ (ms)	↓	↑
Cm (pF)	NC	NC
Passive Electrical Properties LTMR:		
Em (mV)	↑	↑
Ri (MΩ)	NC	NC
τ (ms)	↓	↑
Cm (pF)	NC	↑